OPEN ACCESS Freely available online

PLOS ONE

Group VIB Calcium-Independent Phospholipase A_2 (iPLA$_2\gamma$) Regulates Platelet Activation, Hemostasis and Thrombosis in Mice

Emiko Yoda[1], Kohmi Rai[1], Mai Ogawa[1], Yuki Takakura[1], Hiroshi Kuwata[1], Hidenori Suzuki[2], Yoshihito Nakatani[1], Makoto Murakami[3], Shuntaro Hara[1]*

1 Division of Health Chemistry, Department of Healthcare and Regulatory Sciences, School of Pharmacy, Showa University, Shinagawa-ku, Tokyo, Japan, **2** Division of Morphological and Biomolecular Research, Graduate School of Medicine, Nippon Medical School, Bunkyo-ku, Tokyo, Japan, **3** Lipid Metabolism Project, Tokyo Metropolitan Institute of Medical Science, Setagaya-ku, Tokyo, Japan

Abstract

In platelets, group IVA cytosolic phospholipase A_2 (cPLA$_2\alpha$) has been implicated as a key regulator in the hydrolysis of platelet membrane phospholipids, leading to pro-thrombotic thromboxane A_2 and anti-thrombotic 12-(*S*)-hydroxyeicosatetranoic acid production. However, studies using cPLA$_2\alpha$-deficient mice have indicated that other PLA$_2$(s) may also be involved in the hydrolysis of platelet glycerophospholipids. In this study, we found that group VIB Ca^{2+}-independent PLA$_2$ (iPLA$_2\gamma$)-deficient platelets showed decreases in adenosine diphosphate (ADP)-dependent aggregation and ADP- or collagen-dependent thromboxane A_2 production. Electrospray ionization mass spectrometry analysis of platelet phospholipids revealed that fatty acyl compositions of ethanolamine plasmalogen and phosphatidylglycerol were altered in platelets from iPLA$_2\gamma$-null mice. Furthermore, mice lacking iPLA$_2\gamma$ displayed prolonged bleeding times and were protected against pulmonary thromboembolism. These results suggest that iPLA$_2\gamma$ is an additional, long-sought-after PLA$_2$ that hydrolyzes platelet membranes and facilitates platelet aggregation in response to ADP.

Citation: Yoda E, Rai K, Ogawa M, Takakura Y, Kuwata H, et al. (2014) Group VIB Calcium-Independent Phospholipase A_2 (iPLA$_2\gamma$) Regulates Platelet Activation, Hemostasis and Thrombosis in Mice. PLoS ONE 9(10): e109409. doi:10.1371/journal.pone.0109409

Editor: Toshiyuki Miyata, National Cerebral and Cardiovascular Center, Japan

Received June 16, 2014; **Accepted** August 31, 2014; **Published** October 14, 2014

Data Availability: The authors confirm that all data underlying the findings are fully available without restriction. All relevant data are within the paper and its Supporting Information files.

Funding: This work was in part by a Grant-in-Aid for Scientific Research (B) (21390036 and 25293033) and a Grant-in-Aid for Research Activity start-up (21890254) from the Japan Society for the Promotion of Science; by a Grant-in-Aid for Scientific Research on Innovative Areas (25116720) and a grant for Private University High Technology Research Center Project from the Ministry of Education, Sports, Science, Culture and Technology of Japan; and by a grant from the Terumo Life Science Foundation. The funders had no role in study design, data collection and analysis, decision to publish, or preparation of the manuscript.

Competing Interests: The authors have declared that no competing interests exist.

* Email: haras@pharm.showa-u.ac.jp

Introduction

Platelets play a key role in hemostasis through their ability to respond to vascular injury. When circulating platelets are exposed to collagen-rich subendothelium at the site of a vascular injury, platelets become activated, release granule contents, and generate thrombin and the lipid mediator thromboxane A_2 (TXA_2) [1,2]. Secreted adenosine diphosphate (ADP), serotonin, and TXA_2 amplify the initial stimulus in a positive feedback activation of platelets. In addition, α-granule proteins, such as P-selectin, which mediate adhesive interactions between platelets, leukocytes, and endothelial cells, play a pivotal role in the pathogenesis of thrombosis and inflammation [2,3]. TXA_2 is a potent platelet agonist and an arachidonic acid (AA) metabolite, produced via the cyclooxygenase (COX) pathway [4,5]. Another platelet-derived lipid mediator, 12(*S*)-hydroxyeicosatetraenoic acid (12(*S*)-HETE), is also an AA metabolite produced via platelet-type 12-lipoxygenase and acts as a platelet antagonist [6,7]. TXA_2 formation is rapid and quickly reaches a plateau in activated platelets, whereas 12(*S*)-HETE formation is slower and continues to increase over a longer period of time.

AA is released from the *sn*-2 position of glycerophospholipids by the action of phospholipase A_2 (PLA_2). PLA_2 enzymes have been classified into six major families: secretory PLA_2 ($sPLA_2$), cytosolic PLA_2 ($cPLA_2$), Ca^{2+}-independent PLA_2 ($iPLA_2$), platelet-activating factor acetylhydrolases, lysosomal PLA_2s and adipose-specific PLA_2; each family occurs as multiple isoforms [8]. Platelets are known to contain both cPLA$_2\alpha$ (also known as group IVA PLA_2), a $cPLA_2$ enzyme that requires micromolar concentrations of intracellular Ca^{2+} for translocation to membrane phospholipids, and group IIA $sPLA_2$ ($sPLA_2$-IIA), an $sPLA_2$ enzyme that requires millimolar Ca^{2+} concentrations for its enzymatic activity [8]. AA production in platelets is dependent on cPLA$_2\alpha$ but not on $sPLA_2$-IIA [9]. A functional deficiency of cPLA$_2\alpha$ diminished platelet aggregatory and secretory responses to collagen [10]. cPLA$_2\alpha$-deficient mice have prolonged bleeding times and are resistant to thromboembolism induced by injection of a mixture of ADP and collagen, indicating a role of this enzyme in platelet adhesive and hemostatic functions. However, residual AA release and TXA_2 production were still observed in collagen- or ADP-stimulated platelets isolated from cPLA$_2\alpha$/$sPLA_2$-IIA double-deficient mice. Furthermore, bromoenol lactone (BEL), an $iPLA_2$ inhibitor,

inhibits AA production in 12-*O*-tetradecanoylphorbol-13-acetate (PMA)- or thrombin-stimulated platelets [11,12]. These reports have suggested that another PLA_2 enzyme, possibly BEL-sensitive $iPLA_2$ enzyme(s), may compensate for platelet activation.

To date, nine members of the $iPLA_2$ family, also referred to as the patatin-like phospholipase-domain containing (PNPLA) family, have been identified. These $iPLA_2$ isoforms have one or more nucleotide-binding motif (GXGXXG) and a lipase consensus site (GXSXG) separated by a 10–40-amino acid residue spacer linkage [13,14]. Unlike $cPLA_2$s and $sPLA_2$s, $iPLA_2$s do not require intracellular Ca^{2+} for enzymatic activity or membrane binding, and they are sensitive to BEL [15–17]. Among $iPLA_2$s, it is assumed that two abundant isoforms –iPLA$_2\gamma$/PNPLA8 (group VIB) and iPLA$_2\beta$/PNPLA9 (group VIA)– serve as housekeeping enzymes responsible for phospholipid acyl group turnover and generation of the lysophospholipids necessary for AA incorporation [14,18,19].

Recently, several studies have revealed the role of iPLA$_2\gamma$ in lipid mediator production. For example, overexpression of iPLA$_2\gamma$ has been shown to promote spontaneous and agonist-stimulated release of AA, which is converted to prostaglandin E_2 (PGE_2) with preferred COX-1 coupling in HEK293 cells [20]. The induction of group IIA $sPLA_2$ by pro-inflammatory stimuli has been shown to require iPLA$_2\gamma$ through production of certain lipid metabolite(s) in rat fibroblastic 3Y1 cells [21]. iPLA$_2\gamma$ could produce 2-arachidonoyl-lysophosphatidylcholine, a presumptive lipid mediator, through its PLA_1 action [22]. In addition, disruption of the iPLA$_2\gamma$ gene in mice reduced the levels of prostaglandin $F_{2\alpha}$ ($PGF_{2\alpha}$) and D_2 (PGD_2) in skeletal and heart muscle and those of TXA_2 in heart muscle [23]. Moreover, Ca^{2+}-induced myocardial activation of iPLA$_2\gamma$ and the attendant release of AA and its metabolites, were attenuated by genetic ablation of iPLA$_2\gamma$ [24]. These results raise the possibility that iPLA$_2\gamma$ may be involved in AA release from glycerophospholipids in activated platelets.

In the current study, we investigated the role of iPLA$_2\gamma$ in platelets using iPLA$_2\gamma$ knockout (iPLA$_2\gamma$-KO) mice. Our findings demonstrate that lack of iPLA$_2\gamma$ expression *in vivo* increased bleeding time and protected mice from thromboembolism. In studies using isolated platelets, iPLA$_2\gamma$-KO mouse platelets were aggregated only poorly, and produced a reduced level of TXA_2 in response to ADP. Furthermore, electrospray ionization mass spectrometry (ESI-MS) analysis of platelet phospholipids suggested that iPLA$_2\gamma$ mainly catalyzed the hydrolysis of AA-containing plasmalogen-type phosphatidylethanolamine (PE) and phosphatidylglycerol (PG) and subclasses in activated platelets. These results indicate that, together with cPLA$_2\alpha$, iPLA$_2\gamma$ plays a role in AA mobilization from specific AA-containing phosholipid pools in activated platelets.

Materials and Methods

Antibodies and Reagents

The study used iPLA$_2\gamma$-KO mice on a C57BL/6j background, as described in a previous study [23]. All procedures involving animals were approved by the Institutional Animal Care and Use Committees of Showa University. ADP, prostaglandin E_1 (PGE_1), thrombin and anti-β-actin monoclonal antibody were purchased from Sigma (St Louis, MO). U46619 and AA were from Cayman Chemical (Ann Arbor, Michigan). Collagen reagent Horm (native collagen fibrils from equine tendons) was purchased from Nycomed Arzneimittel (Munchen, Germany). MRS2365 and MRS2279 were purchased from TOCRIS bioscience (Bristol, UK). Phosphatidylcholine (PC) with $C_{28:0}$, PE with $C_{28:0}$ and PG with $C_{28:0}$ were from Avanti Polar Lipids, Inc. (Alabaster, AL). Paraformaldehyde, glutaraldehyde, EPON, and uranyl acetate were obtained from TAAB Laboratories (Aldermaston, West Berkshire, UK). Rabbit anti-adenylyl cyclase (AC), phosphodiesterase (PDE) 3A and PDE5 polyclonal antibody, anti-cPLA$_2\alpha$ monoclonal antibody and goat anti-COX-1 and $G_{\alpha i}$ antibody were purchased from Zymed Laboratories (South San Francisco, CA). Rabbit anti-iPLA$_2\gamma$ polyclonal antibody was prepared as described in previous studies [21,23].

Isolation of Platelets

Mice anesthetized with diethyl ether were used for cardiac puncture. The heart was exposed and a 1-ml syringe with a 25-gauge needle containing 100 µl of 3.8% (w/v) trisodium citrate was used to obtain about 1 ml of blood. The platelet-rich plasma (PRP) was obtained by centrifugation of whole blood at $250\times g$ for 10 min at room temperature, platelet-poor plasma (PPP) was obtained by centrifugation of lower-phase blood at $800\times g$ for 15 min at room temperature, and PRP were diluted by PPP at a concentration of 200×10^3/µl for ADP, MRS2365 or MRS2279 stimulation. For ADP, collagen, thrombin, PMA, AA or A23187 stimulation, platelets were isolated by differential centrifugation from PRP, then were suspended in HEPES/tyrode's (H/T) buffer (pH 7.35) [138 mM NaCl, 2.8 mM KCl, 3.75 mM $NaH_2PO_4\cdot12H_2O$, 0.8 mM $MgCl_2$, 10 mM HEPES, 5.6 mM dextrose, 0.35% (w/v) bovine serum albumin], supplemented with 1 µM PGE_1. Platelet suspension was incubated for 15 min at 37°C and centrifuged at $800\times g$ for 15 min at room temperature. Final platelet suspension was adjusted to 200×10^3/µl with H/T buffer without PGE_1.

Platelet Aggregation

Platelet aggregation (180 µl samples) was assessed in an aggregometer (HEMA tracer, LMS Co., Ltd., Tokyo, Japan) with constant stirring (100 rpm) at 37°C. The platelets were then incubated with various inhibitors, and without stirring, at 37°C, for various periods of time before agonists were added: collagen (1 µg/ml), ADP (10 µM), U46619 (5 µM), thrombin (0.1 U/ml), A23187 (5 µM), AA (100 µM), PMA (10 nM), MRS2365 (10 µM) and MRS2279 (10 µM). Aggregation was measured and expressed as a percent change in light transmission, with the value for blank sample (PPP or H/T buffer without platelets) set at 100%.

SDS-PAGE and Immunoblotting

Ten-µg protein was subjected to SDS-PAGE using 7.5% or 12% gels under reducing conditions. The separated proteins were electroblotted onto nitrocellulose membranes (Schleicher & Schuell, Dassel, Germany) with a semidry blotter (Bio-Rad Laboratories, Hercules, USA) according to the manufacturer's instructions. After blocking with 5% (w/v) skim milk in 10 mM Tris-HCl, pH 7.4, containing 150 mM NaCl and 0.05% Tween 20, membranes were probed with the respective antibodies (1:5,000 dilution for iPLA$_2\gamma$ COX-1, $P2Y_1$, $P2Y_{12}$, AC, PDE3A, PDE5 and $G_{\alpha i}$; 1:10,000 dilution for cPLA$_2\alpha$ and β-actin) for 1 h, then incubated with horseradish peroxidase-conjugated anti-rabbit (1:5,000 for iPLA$_2\gamma$ $P2Y_1$, $P2Y_{12}$, AC, PDE3A and PDE5) IgG, peroxidase-conjugated anti-goat (1:5,000 for COX-1 and $G_{\alpha i}$) IgG and peroxidase-conjugated anti-mouse (1:10,000 for cPLA$_2\alpha$ and β-actin) IgG. After washing, the membranes were visualized with Western Lightning Chemiluminescence Reagent Plus (Perkin Elmer Life Sciences, Boston, MA, USA).

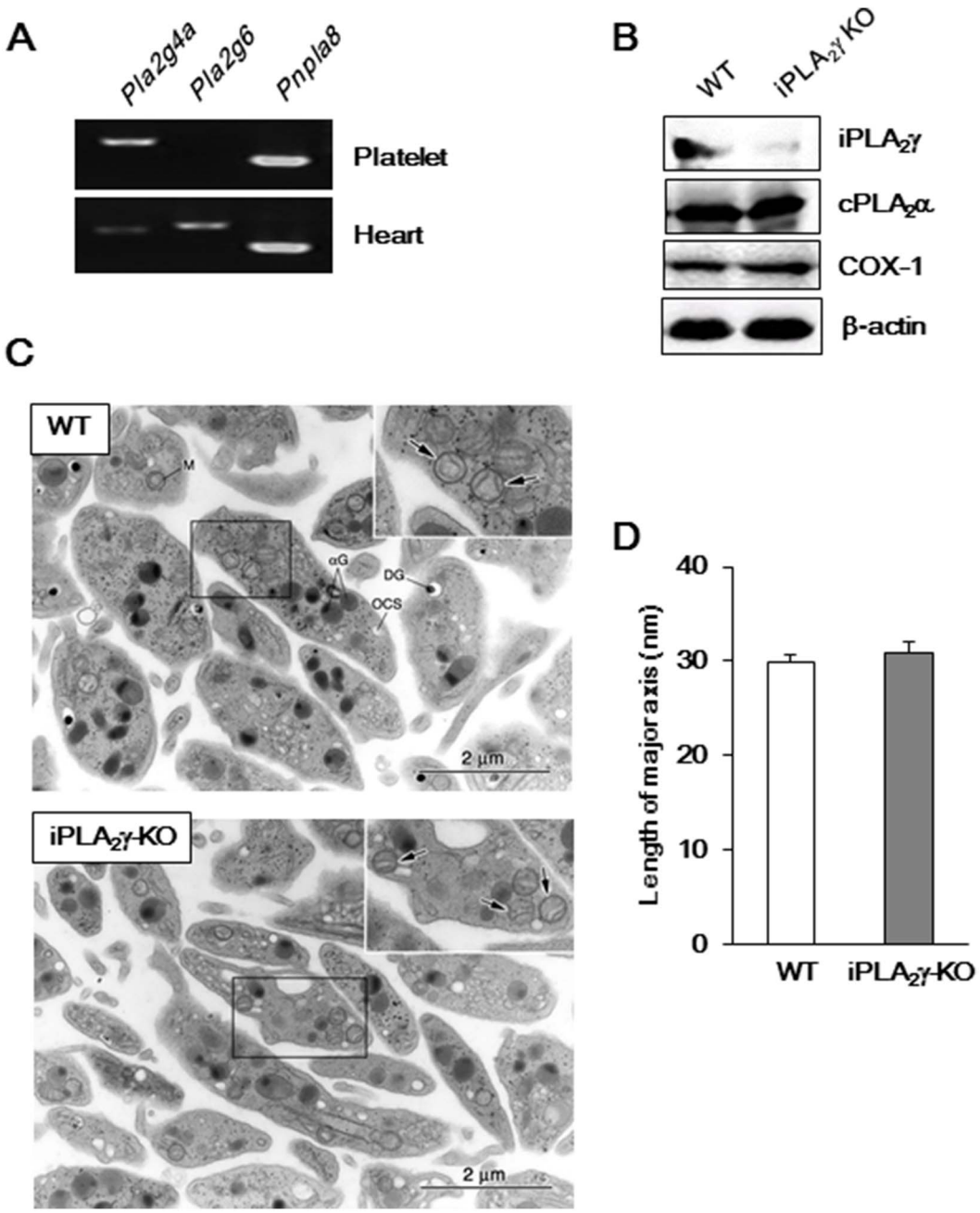

Figure 1. Expression of iPLA$_2\gamma$ in platelets and morphological features of iPLA$_2\gamma$-KO mouse platelets. (A) RT-PCR analysis of cPLA$_2\alpha$ (Pla2g4a), iPLA$_2\beta$ (Pla2g6) and iPLA$_2\gamma$ (Pnpla8) mRNA expressions in platelets (upper panel) and heart (lower panel). (B) Immunoblot analysis of iPLA$_2\gamma$ cPLA$_2\alpha$ and COX-1 expression in WT and iPLA$_2\gamma$-KO platelets. β-actin was used as a loading control. (C) Images of WT (upper panel) and iPLA$_2\gamma$-KO platelet (lower panel) ultrastructure obtained by electron microscopy. M, mitochondrion; OCS, open canalicular system; αG, α-granules; DG, dense granule. Boxed areas are magnified in the upper right corners. Arrows indicate mitochondria. Representative results of at least three experiments are shown (A–C). (D) The length of the major axis of mitochondria in platelets from WT (open column) and iPLA$_2\gamma$-KO mice (closed column). Results are the average length (nm) ±SEM (n = 3).
doi:10.1371/journal.pone.0109409.g001

Reverse Transcription PCR

Total RNA was extracted from mouse platelets with TRIzol reagent (Invitrogen Life Technologies, Carlsbad, CA, USA). First-strand cDNA synthesis was conducted using the SuperScript III reverse transcriptase kit (Invitrogen Life Technologies) according to the manufacture's instructions. Five μg of total RNA in reaction mixture was primed with oligo (dT) (12–18 mer) primer (Invitrogen Life Technologies) to obtain cDNA. Then, 1 ml of the synthesized cDNA was used as the template for the mRNA amplification reactions. The PCR conditions were 96°C for 5 min, then 35 cycles of 96°C and 63°C for 30 s, and finally 68°C for 2 min on a thermal cycler (Applied Biosystetms). The reverse transcription PCR products were analyzed by 1% agarose gel electrophoresis with ethidium bromide. The primer pairs were *Pla2g4a* (forward: 5′- gcatggcactgtgtgatcag-3′, reverse: 5′-cgtgaa-gagaggcaaaggaca-3′); *Pla2g6* (forward: 5′-gcaaacactggcactctc-

Table 1. Hematological parameters of WT and iPLA$_2\gamma$-KO mice.

	WT	iPLA$_2\gamma$-KO
Platelets ($\times10^3$/μl)	598.17±101.76	530.67±114.17
White blood cells ($\times10^3$/μl)	10.06±0.92	8.44±0.99
Red blood cells ($\times10^6$/μl)	10.03±0.38	10.28±0.51
Hematocrit (%)	45.73±1.68	46.17±1.88
Hemoglobin (g/dl)	14.80±0.62	15.37±0.82
MPV (fl)	7.13±0.13	7.10±0.14

Data are mean±SEM. No abnormalities or significant differences between WT and iPLA$_2\gamma$-KO mice were observed for hematologic parameters (n = 4–5).
MPV indicates mean platelet volume.
doi:10.1371/journal.pone.0109409.t001

caag-3′, reverse: 5′-cggagaatgactccaaatctgg-3′); *Pnpla8* (forward: 5′-gagactgccttccattacgct-3′, reverse: 5′-tcgtttggggtgtccacttc-3′).

Electron Microscopy

The platelets suspended in H/T buffer were fixed by mixing with an equal volume of 2% glutaraldehyde in 0.1 M phosphate buffer (PB, pH 7.4) for 30 min at room temperture. The fixed cells were transferred to eppendorf tubes, then centrifuged at 2,000 rpm for 5 min at 4°C. The platelet pellets were dissected into blocks of 1-mm cubes, washed 5 times in 0.1 M PB, post-fixed with 1% osmium tetroxide in the same buffer for 1 h at 4°C, dehydrated with a graded ethanol series, and then embeded in Epon 812, according to the conventional method. Ultra-thin sections were cut with a diamond knife and stained with uranyl acetate and lead citrate, then examined with a JEM-1200EX electron microscope (JEOL, Tokyo, Japan) at an accelerating voltage of 80 kV.

Measurement of ATP and Serotonin Secretion

After the reaction, platelets were removed by centrifugation in the presence of 5 mM of ice cold EDTA and 10 μg/ml indomethacin. The amounts of adenosine triphosphate (ATP) and serotonin in platelet-free supernatant fraction was measured using an ATP bioluminescence assay kit CLS II (Roche Applied Science, Mannheim, Germany) and EIA Serotonin kit (IMMUNOTECH SAS, Marseille, France), respectively, according to the manufacturer's protocol.

Ca^{2+} Influx

Washed platelets were loaded with fura-2 by incubation in RPMI1640 medium containing 5 μM fura-2/AM (Dojindo Laboratories, Kumamoto, Japan), PGE_1 and 10% fetal bovine serum at 37°C for 40 min. The fura-2-loaded platelets were washed with H/T buffer (pH 7.35) containing PGE_1 twice and resuspended in loading solution (145 mM NaCl, 10 mM HEPES, 10 mM $MgCl_2$, 6 mM glucose, 5 mM KCl (pH 7.35)) at a

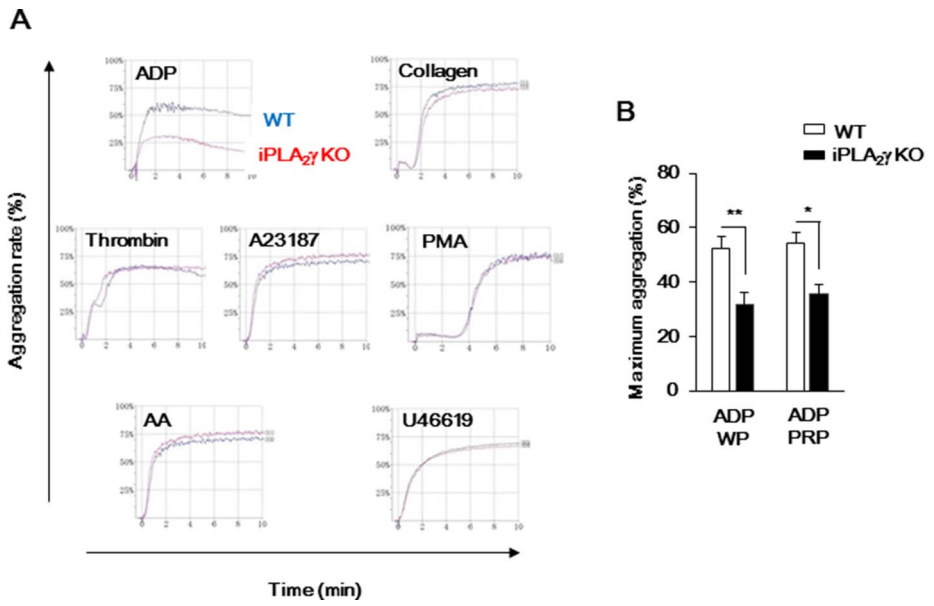

Figure 2. iPLA$_2\gamma$ deficiency inhibits platelet aggregation in response to ADP stimulation. (A) Representative results from aggregometry testing. Washed platelets from WT (blue) or iPLA$_2\gamma$-KO (red) mice were stimulated with the indicated agonists (ADP (10 μM), collagen (1 μg/ml), thrombin (0.1 U/ml), A23187 (5 μM), PMA (10 nM), AA (100 μM) or U46619 (5 μM)), and then light transmission was recorded on an aggregometer. (B) Bar graphs indicate results obtained by aggregometry tests. Washed platelets (WP) or platelets in PRP (200×10^3/μl) from WT or iPLA$_2\gamma$-KO mice were stimulated with ADP (10 μM), and then light transmission was recorded on an aggregometer. Results are given as the mean percentage of maximum aggregation±SEM (n = 6–10). *$P<0.05$ and **$P<0.01$ between iPLA$_2\gamma$-KO and WT.
doi:10.1371/journal.pone.0109409.g002

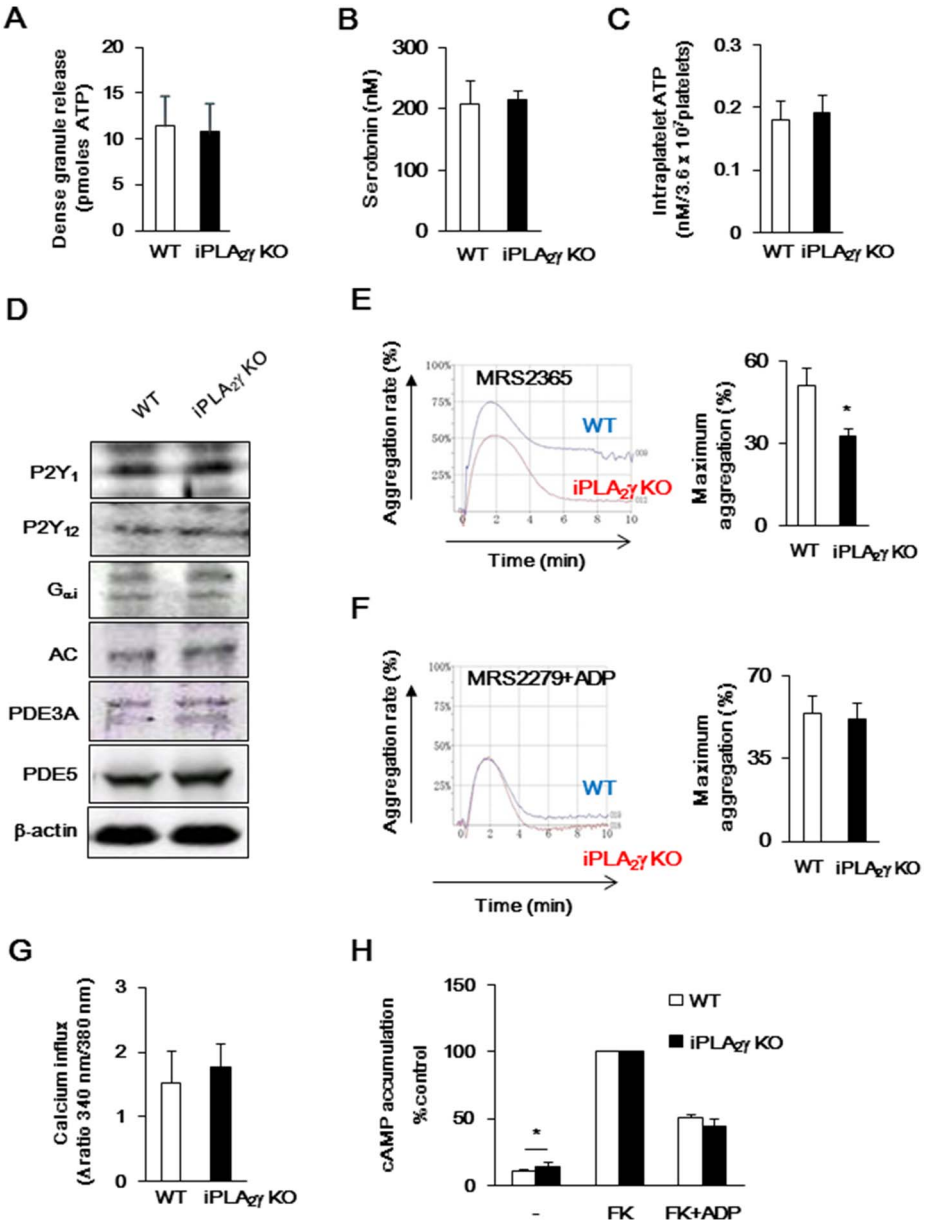

Figure 3. P2Y receptors-mediated signaling of iPLA$_2\gamma$ deficient platelets. (A and B) Dense granule secretion was evaluated by measuring ATP (A) and serotonin (B) release after the ADP aggregation of WT (open columns) or iPLA$_2\gamma$-KO (closed columns) platelets. Results are expressed as the amounts of ATP (n = 10–13) and serotonin (n = 3–4) released by 3.6×10^7 from platelets. (C) Measuring intraplatelet ATP levels of resting state of WT (open columns) or iPLA$_2\gamma$-KO (closed columns) platelets (n = 5). (D) Protein expression of P2Y$_1$, P2Y$_{12}$, G$_{\alpha i}$, AC and PDEs of platelets from WT and iPLA$_2\gamma$-KO mice. β-actin was used as a loading control. Representative results of at least three experiments are shown. (E and F) PRP from WT (blue) or iPLA$_2\gamma$-KO (red) mice were stimulated with P2Y$_1$ agonist (MRS2365) (10 μM) (E) or P2Y$_1$ antagonist (MRS2279) (10 μM) plus ADP (10 μM) (F), and then light transmission was recorded on an aggregometer. Left panel indicates representative results from aggregometry testing. Right graphs indicate results obtained by aggregometry tests. Results are given as the mean percentage of maximum aggregation±SEM (n = 6–10). *$P<0.05$ between iPLA$_2\gamma$-KO and WT. (G) Ca^{2+} influx of WT (open columns) or iPLA$_2\gamma$-KO (closed columns) platelets in response to ADP (10 μM). Results are given as mean±SEM (n = 8). (H) PRP (200×10^3/μl) from WT (open columns) or iPLA$_2\gamma$-KO (closed columns) was incubated both with and without forskolin (FK; 5 μM) for 30 s before ADP (10 μM) was added and the samples were incubated for 5 min at room temperature. Results are given as the mean±SEM (n = 5). *$P<0.05$ between iPLA$_2\gamma$-KO and WT.
doi:10.1371/journal.pone.0109409.g003

concentration of 200×10^3/μl, then activated with 10 μM ADP. Fluorescence was continuously recorded using CAF-110 (JASCO Co., Ltd., Tokyo, Japan) at 37°C by alternating the excitation wavelength between 340 and 380 nm, and detecting the fluorescent emission at 510 nm with the bandwidth set at 2.5 nm for both emission and excitation.

Analysis of Intraplatelet cAMP Levels

PRP (200×10^3/μl) was incubated both with and without forskolin (FK) for 30 s before ADP was added and the samples were incubated for 5 min at room temperature. FK stimulates AC and then increase intraplatelet cAMP levels. The reaction was stopped by the addition of 50 μl of ice-cold 30% (v/v) trichloroacetic acid. Samples were mixed and centrifuged at

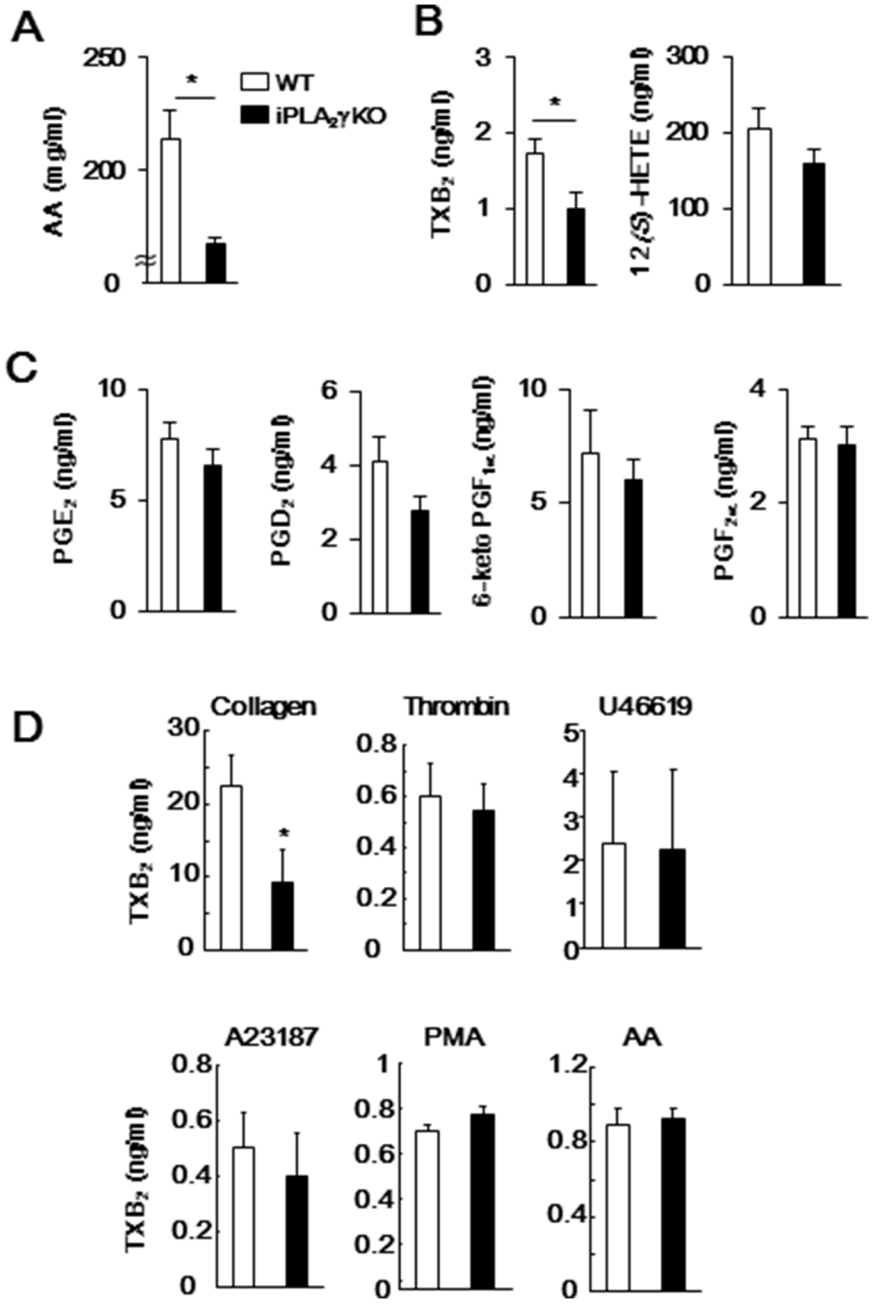

Figure 4. Amounts of lipid mediators produced from WT and iPLA$_2\gamma$-KO mouse platelets after ADP stimulation. Levels of (A) AA, (B) TXB_2 (a TXA_2 metabolite) and 12*(S)*-HETE, and (C) PGE_2, PGD_2, 6-keto prostaglandin $F_{1\alpha}$ (6-ketoPGF$_{1\alpha}$) (a prostacyclin metabolite) and prostaglandine $F_{2\alpha}$ (PGF$_{2\alpha}$) in supernatants from WT (open columns) or iPLA$_2\gamma$-KO (closed columns) platelets stimulated with ADP (10 μM). (D) Levels of TXB_2 in supernatants from WT (open columns) or iPLA$_2\gamma$-KO (closed columns) mouse platelets stimulated with collagen (1 μg/ml), thrombin (0.1 U/ml), A23187 (5 μM), PMA (10 nM), AA (100 μM) or U46619 (5 μM). Results are given as mean±SEM (n = 3–9). *$P<0.05$ between iPLA$_2\gamma$-KO and WT.
doi:10.1371/journal.pone.0109409.g004

6,000×g for 20 min at 4°C. Supernatants were removed and retained, and the pH was neutralized by addition of 8 mM KOH. Samples were stored at −80°C and assayed for cAMP using Amersham cAMP Biotrak EIA system (GE healthcare, UK) according to the manufacturer's instructions.

ESI-MS Analysis of Phospholipids

Platelets (3.6×10^7 cells) were soaked in 200 μl of H_2O and then sonicated for 30 s. Lipids were extracted from the lysates using the method described in Bligh and Dyer [25]. Before lipid extraction, PC with $C_{28:0}$ (14:0–14:0; m/z = 678), PE with $C_{28:0}$ (14:0–14:0; m/z = 635) and PG with $C_{28:0}$ (14:0–14:0; m/z = 666) were added to each sample as an internal standard (2 nmol per tissue) (Avanti Polar Lipids, Inc.). The analysis was performed using a 5500Q–TRAP quadrupole-linear ion trap hybrid mass spectrometer (Applied Biosystems/MDS Sciex) with an Ultimate 3000 HPLC system (Shimadzu Science, Kyoto, Japan). The extracted lipids were subjected to ESI-MS analysis by flow injection with liquid chromatography separation. The mobile phase composition was acetonitrile/methanol/water (18/11/1, v/v/v) (plus 0.1% ammo-

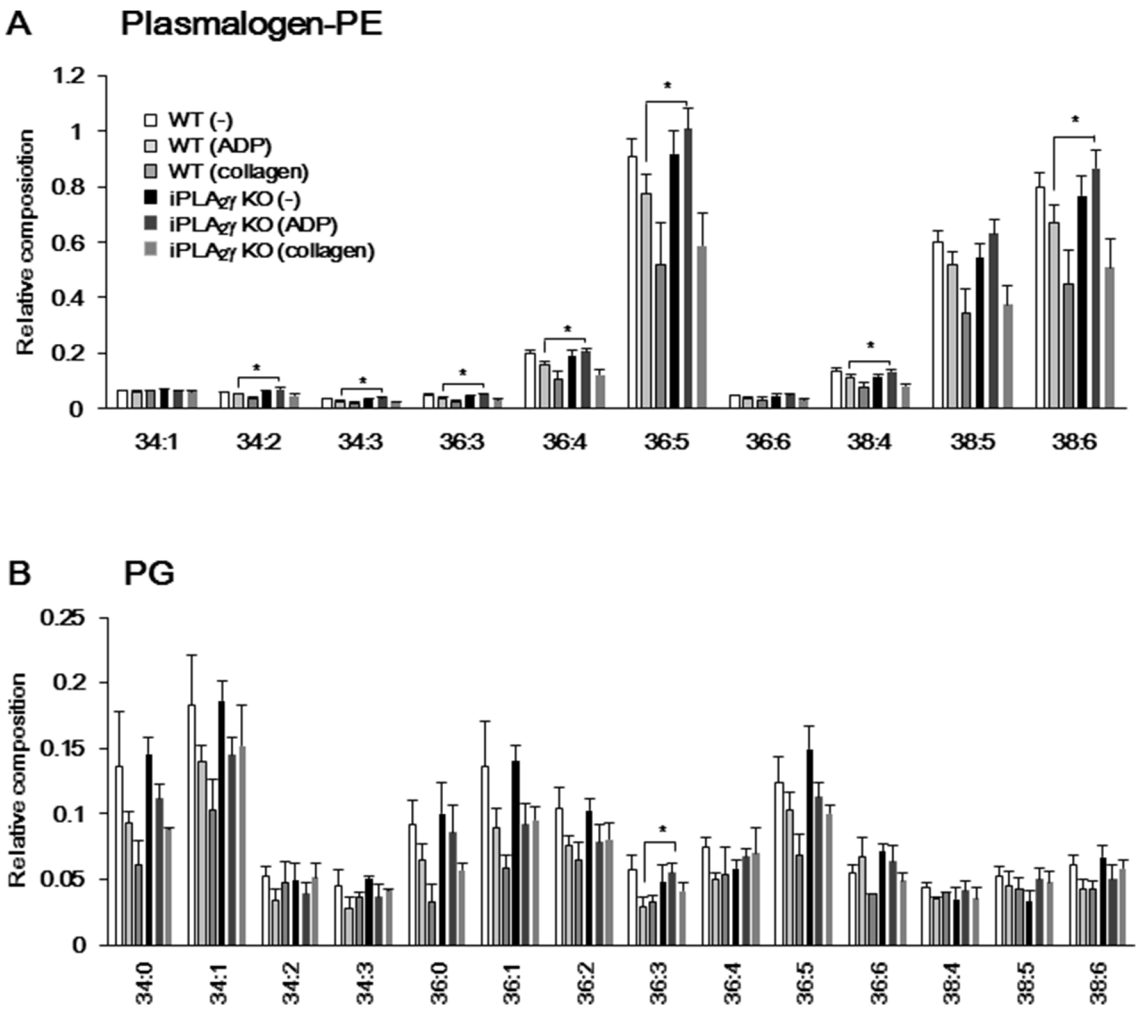

Figure 5. ESI/MS analysis of plasmalogen-PE and PG species in WT and iPLA$_2\gamma$-KO mouse platelets. Total lipids were extracted from resting or ADP (10 μM)-stimulated platelet lysates and then subjected to ESI/MS analysis of PG and PE. Levels of (A) plasmalogen-PE and (B) PG in resting state of WT (–) or iPLA$_2\gamma$-KO platelets (–), or ADP-stimulated WT (ADP) or iPLA$_2\gamma$-KO platelets (ADP), and collagen (1 μg/ml)-stimulated WT (collagen) or iPLA$_2\gamma$-KO platelets (collagen) (n = 7). Results are given as mean±SEM. *$P<0.05$ between iPLA$_2\gamma$-KO and WT.
doi:10.1371/journal.pone.0109409.g005

nium formate (pH 6.8)) at a flow-rate of 10 μl/min. The scan range of the instrument was set at m/z 400–1000, with a scan speed of 10000 Da/s. The trap fill-time was set at 20 ms in the negative-ion mode. The ion spray voltage was set at 5500 V in the negative-ion mode. Nitrogen was used as curtain gas (setting of 20, arbitrary units) and as collision gas (set to "high"). The declustering potential was set at 60 V in the negative-ion mode. The collision energy in ESI-MS and ESI-MS/MS analyses were optimized according to the requirements of the experiment.

Mediator Lipidomics

After 10 min of reaction, platelets were removed by centrifugation in the presence of 5 mM of ice cold EDTA and 10 μg/ml indomethacin. The platelet-free supernatant fraction was used for mediator lipidomics. Mediator lipidomics was performed as described previously [26]. Before eicosanoids extraction, 0.1 ng of prostaglandin B_2 (GE Healthcare) was added to each sample as an internal standard. Then, 0.2% (v/v) formic acid and ethyl acetate were added to each sample before centrifugation. Supernatants were removed and used for ESI-MS/MS analysis with a 5500Q–TRAP quadrupole-linear ion trap hybrid mass spectrometer with an Ultimate 3000 HPLC system and TSKgel ODS-100V C18 column (5 μm, 4.6×150 mm; Tosoh Bioscience, Tokyo, Japan). Samples were eluted with a mobile phase composed of water/acetonitrile/formic acid (63:37:0.02) and acetonitrile/isoplopanol (50:50) 73:23, for 5 min, ramped to 30:70 after 15 min, ramped to 20:80 after 25 min and held for 8 min, then ramped to 0:100 after 35 min and held for 10 min, with flow rates of 70 ml/min (0–30 min), 80 ml/min (30–33 min), and 100 ml/min (33–45 min). ESI-MS/MS analyses were conducted in negative ion mode, and eicosanoids were indicated and quantified by multiple reaction monitoring (MRM). Calibration curves (1–1000 pg) and LC retention times for each compound were established with synthetic standards.

Bleeding Time Measurement

Bleeding time was assessed according to a previously reported method [10]. In brief, 8~9-wks of age male mice were restrained in the upright position and their tails were transected 5 mm proximal from the tip. The remaining tail was then immersed in saline at 37°C. Bleeding time was defined as either the point at

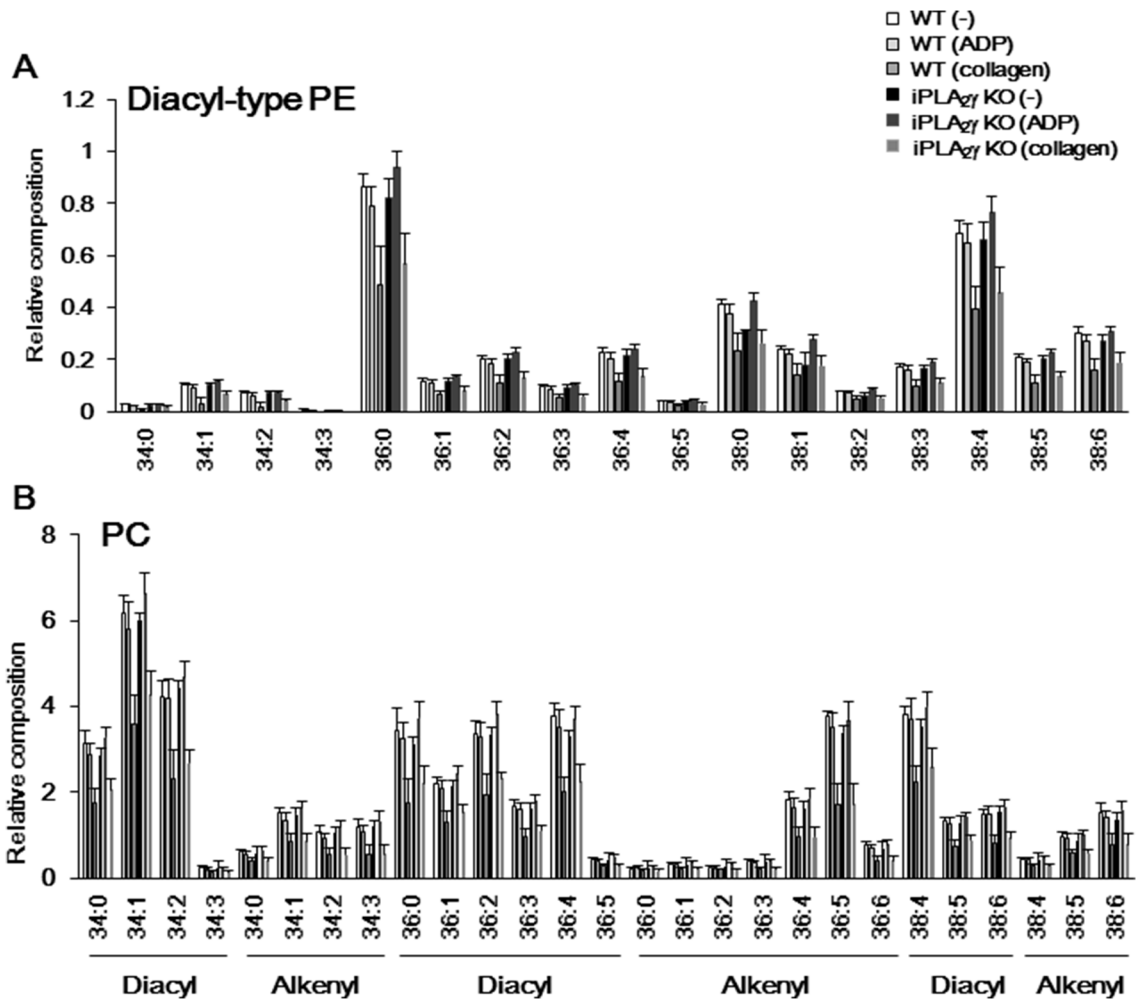

Figure 6. ESI/MS analysis of diacyl-type PE and PC species in WT and iPLA$_2\gamma$-KO mouse platelets. Total lipids were extracted from resting or ADP (10 μM)-stimulated platelet lysates and then subjected to ESI/MS analysis of diacyl-type PE and PC. Levels of (A) diacyl-type PE and (B) PC in resting state of WT (–) or iPLA$_2\gamma$-KO platelets (–), or ADP-stimulated WT (ADP) or iPLA$_2\gamma$-KO platelets (ADP), and collagen (1 μg/ml)-stimulated WT (collagen) or iPLA$_2\gamma$-KO platelets (collagen) (n = 7). Results are given as mean±SEM.
doi:10.1371/journal.pone.0109409.g006

which all visible signs of bleeding from the incision stopped, or at 10 min.

Thromboembolism Test

The tail veins of mice anesthetized with 5 mg/kg sodium pentbarbital were injected with 0.25 mg/kg collagen and 20 mg/kg of epinephrine dissolved in a buffer. Survival was evaluated 1 h after injection. Statistical analysis between WT and iPLA$_2\gamma$-KO groups was assessed by Fisher's exact test. The amount of collagen and epinephrine used was determined as that which induced mortality of 80%–90% in wild-type (WT) mice. For histological examination, mice were killed 2 min after injection, the heart was exposed and a 1-ml syringe with a 25-gauge needle containing EDTA powder was used to obtain about 200 μl of blood. The plasma was obtained by centrifugation of whole blood at 10,000×*g* for 15 min at 4°C, and the lungs were excised. Tissue preparations were stained with hematoxylin and eosin, and the lungs were homogenate in 1 ml of methanol. Lipids were extracted from the lysates by the method detailed in Bligh and Dyer. The thromboxane B_2 (TXB_2) contents of serum or lung were then used for ESI-MS/MS analysis.

Data Analysis

Results are shown as mean±SEM from at least three individual experiments per group. Statistical analyses between WT and iPLA$_2\gamma$-KO groups were assessed by student *t* test. *P* values less than 0.05 were considered statistically significant.

Results

iPLA$_2\gamma$ Expression in Murine Platelets and Morphological Features of iPLA$_2\gamma$-Deficient Mouse Platelets

We first examined whether mRNAs for iPLA$_2\beta$ and iPLA$_2\gamma$ were expressed in murine platelets using the RT-PCR method (Figure 1A). Expression of mRNAs for iPLA$_2\gamma$ (*Pnpla8*) and cPLA$_2\alpha$ (*Pla2g4a*) was detected, but not for iPLA$_2\beta$ (*Pla2g6*); meanwhile, the two iPLA$_2$s and, to a lesser extent, cPLA$_2\alpha$ were expressed in the heart used as a positive control. The absence of iPLA$_2\gamma$ protein in the iPLA$_2\gamma$-KO mouse platelets was confirmed by western blot analysis of platelet lysates. The protein levels of COX-1 and cPLA$_2\alpha$ were not significantly different between WT and iPLA$_2\gamma$-KO mouse platelets (Figure 1B). There were no abnormalities in the platelet numbers and mean platelet volume in iPLA$_2\gamma$-KO mice (Table 1). Furthermore, electron microscopy

revealed that resting iPLA$_2\gamma$-KO mouse platelets showed a normal discoid morphology (Figure 1C). Although previous reports showed that iPLA$_2\gamma$-KO mice had abnormal mitochondria in skeletal muscle, myocardium and brain [23,29], mitochondrial architecture was virtually normal in iPLA$_2\gamma$ null mouse platelets. The average length of the major axis of mitochondria in platelets was not significantly affected by iPLA$_2\gamma$ deficiency (Figure 1D).

Reduced ADP-dependent Aggregation of iPLA$_2\gamma$-deficient Mouse Platelets

As shown in Figure 2, functional studies of platelets from iPLA$_2\gamma$-KO mice, compared to WT mice, revealed that ADP-induced aggregation was reduced, whereas aggregation in response to other platelet activators, including collagen, thrombin, Ca^{2+}-ionophore (A23187), PMA, AA and TXA_2 receptor (TP) agonist (U46619) were similar between iPLA$_2\gamma$-KO and WT platelets. Even when PRP was stimulated with ADP, platelet aggregation was also reduced by iPLA$_2\gamma$ deficiency. The release of the contents in platelet-dense granules has been thought to play an important role in perpetuating the aggregation response [1,3]. We therefore investigated the effect of iPLA$_2\gamma$ deletion on ADP-induced dense granule release by quantifying liberated ATP and serotonin. In response to ADP, platelets from iPLA$_2\gamma$-KO mouse secreted ATP and serotonin to levels comparable to those from WT platelets (Figure 3A and B). Moreover, intracellular ATP levels were not significantly different between WT and iPLA$_2\gamma$-deficient mouse platelets (Figure 3C). These results indicated that iPLA$_2\gamma$ deletion affected neither ADP-induced dense granule release nor cellular ATP synthesis, which is consistent with normal mitochondrial morphology in the iPLA$_2\gamma$-KO mice (Figure 1C).

ADP induces platelet aggregation through two G-protein coupled receptors --- G_q-coupled $P2Y_1$, and G_i-coupled $P2Y_{12}$ [28,29]. The protein levels of $P2Y_1$ and $P2Y_{12}$ in iPLA$_2\gamma$-deficient mouse platelets were similar to those in WT platelets (Figure 3D). Like ADP-induced platelet aggregation, $P2Y_1$ agonist MRS2365-induced aggregation was also reduced by iPLA$_2\gamma$ deficiency (Figure 3E). On the other hand, when platelets were pretreated with $P2Y_1$ antagonist MRS2279 and then stimulated with ADP, platelet aggregation from iPLA$_2\gamma$-KO mouse was similar to that of WT platelets (Figure 3F). These results indicated that iPLA$_2\gamma$ is involved in $P2Y_1$-mediated platelet aggregation by ADP stimulation, not $P2Y_{12}$-. $P2Y_1$ receptor stimulation increases intracellular Ca^{2+} levels by phospholipase Cβ activation, and $P2Y_{12}$ receptor stimulation results in $G_{\alpha i}$-mediated inhibition of AC [28,29]. We further examined the effects of iPLA$_2\gamma$ deficiency on ADP-induced second messenger signaling, but our analysis revealed that there was little difference in second messenger signaling between WT and iPLA$_2\gamma$-deficient mouse platelets. ADP-induced increment in intracellular Ca^{2+} levels was not significantly affected by iPLA$_2\gamma$ deficiency (Figure 3G). Notably, intracellular cAMP levels in non-treated iPLA$_2\gamma$-deficient mouse platelet were significantly higher than in WT platelets (Figure 3H), although the protein levels of AC, PDE3A, PDE5 and $G_{\alpha i}$ subunit in iPLA$_2\gamma$-deficient mouse platelets were similar to those in WT platelets (Figure 3D). However, the increased cAMP level in FK-treated iPLA$_2\gamma$-deficient mouse platelets was decreased by ADP stimulation to a level similar to that in WT platelets (Figure 3H).

Lipidomics of Platelets

We further examined the effects of iPLA$_2\gamma$ deletion on AA release and production of AA metabolites by ADP-activated platelets using ESI-MS/MS analysis. Release of AA and TXA_2 (measured as its stable analog, TXB_2) from iPLA$_2\gamma$-deficient mouse platelets was significantly reduced compared to that of WT platelets (Figure 4A and B). Although there were no significant differences between genotypes, the levels of other AA metabolites, such as 12*(S)*-HETE, PGE_2 and PGD_2 also tended to be lower in iPLA$_2\gamma$-KO mouse platelets than in WT mouse platelets (Figure 4B and C). In addition, collagen-induced TXA_2 generation was decreased in iPLA$_2\gamma$-deficient mouse platelets, although TXA_2 generation in response to thrombin, A23187, PMA, AA and U46619 were not significantly different (Figure 4D).

To assess the contribution of iPLA$_2\gamma$ to stimulant-dependent phospholipid hydrolysis in platelets, we performed ESI/MS lipidomics analysis. Interestingly, some specific species of phospholipids, namely alkenyl forms of PE (plasmalogen PE) and PG bearing $C_{18:2}$ (linoleic acid) or $C_{20:4}$ (AA) at the *sn-2* position, were selectively decreased by ADP stimulation in WT platelets, whereas the decrease of these species was not observed in platelets from the iPLA$_2\gamma$-KO mouse (Figure 5). As shown in Figure 5A, many, if not all, of the subclasses of plasmalogen PE, such as those with $C_{34:2}$ ($C_{16:0}$ and $C_{18:2}$), $C_{34:3}$ ($C_{16:1}$ and $C_{18:2}$), $C_{36:3}$ ($C_{18:1}$ and $C_{18:2}$), $C_{36:4}$ ($C_{16:0}$ and $C_{20:4}$), $C_{36:5}$ ($C_{16:1}$ and $C_{20:4}$), $C_{38:4}$ ($C_{18:0}$ and $C_{20:4}$), and $C_{38:6}$ ($C_{18:2}$ and $C_{20:4}$), were decreased by ADP stimulation in WT platelets, whereas the decrease of these species was not observed in iPLA$_2\gamma$-deficient mouse platelets. The plasmalogen PE subclasses with $C_{36:4}$, $C_{36:5}$, $C_{38:4}$, and $C_{38:6}$ were confirmed to contain AA, because a molecular ion peak of *m/z* 303 (= $C_{20:4}$), in addition to that of the corresponding parent ion, was mainly detected on the MS/MS.

On the other hand, all most all of phospholipid subclasses were decreased by collagen stimulation and there was little difference in collagen-induced phospholipid hydrolysis between WT and iPLA$_2\gamma$-KO platelets. As shown in Figure 5B, iPLA$_2\gamma$-deficient mouse platelets in a resting state showed a tendency to contain lower PG subclasses with $C_{36:3}$, $C_{36:4}$, $C_{38:4}$,and $C_{38:5}$ than did WT mouse platelets. These PG species were decreased in WT mouse platelets, but not in iPLA$_2\gamma$-deficient mouse platelets after ADP or collagen stimulation. By contrast, there was no significant difference in composition of the diacyl forms of PE, or in essentially all of the molecular species of PC between WT and iPLA$_2\gamma$-KO (Figure 6). These data suggest that iPLA$_2\gamma$ mainly catalyzes the hydrolysis of plasmalogen PE and PG-bearing $C_{18:2}$ and $C_{20:4}$ in a resting state, or ADP-activated platelets, and that these released AA are metabolized to eicosanoids, including TXA_2.

Impaired Hemostasis and Decreased Susceptibility to Thromboembolism in iPLA$_2\gamma$-deficient Mice

To delineate the role of iPLA$_2\gamma$ in platelet hemostasis and thrombus formation *in vivo*, a tail-bleeding time assay and thromboembolism test were performed. We first found that bleeding times were significantly longer in iPLA$_2\gamma$-KO mice than in gender-matched WT mice (Figure 7A).

Next, WT and iPLA$_2\gamma$-KO mice were intravenously injected with a mixture of collagen and epinephrine, which causes lethal pulmonary thromboembolism. This mouse model is often used to assess ADP-induced platelet activation *in vivo*. In fact, this model had revealed that both $P2Y_1$ genetic deletion and antagonists increased resistance to thrombosis *in vivo* [30,31]. As shown in Figure 7B, histological examination showed marked thrombus formation in the arterioles of the lung in WT mice. Alveolar hemorrhage was also observed in broad areas, frequently accompanying massive pulmonary thrombosis. In contrast, scarce evidence of such thrombus formation or alveolar hemorrhage was found in the lung from iPLA$_2\gamma$-KO mice (Figure 7C). Only 10% of WT mice survived, whereas 50% of iPLA$_2\gamma$-KO mice were still alive 60 min after the challenge (Figure 7D). TXB_2 levels in the

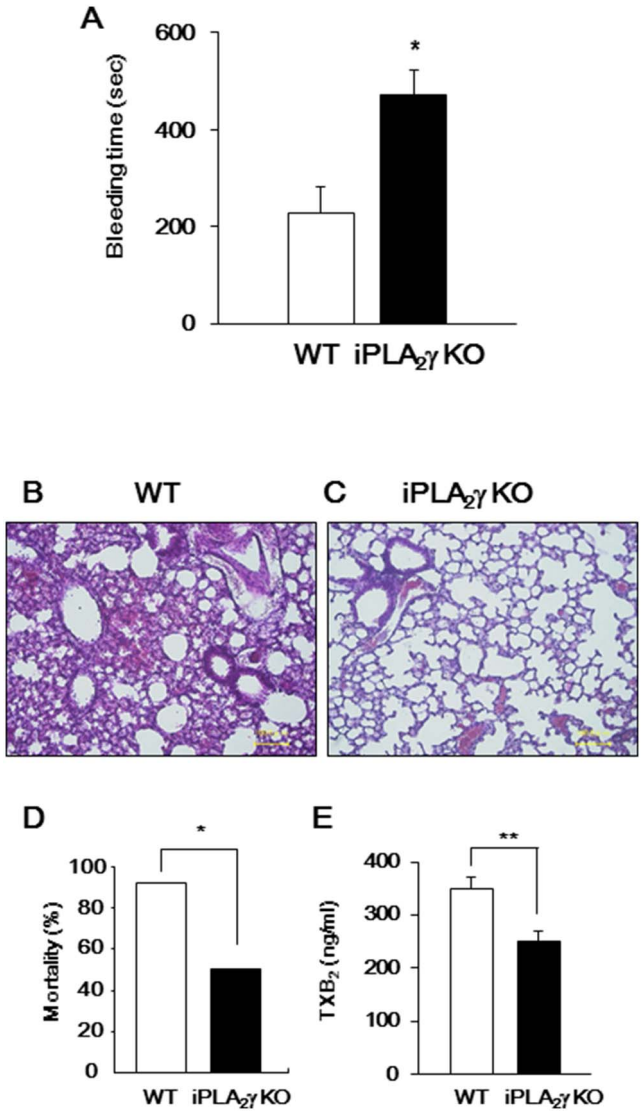

Figure 7. Impaired hemostasis and thrombus formation in iPLA$_2$γ-KO mice. (A) Bleeding times for WT (open column; n = 9) and iPLA$_2$γ-KO (closed column; n = 11) mice. Data are mean±SEM. **P<0.01 between iPLA$_2$γ-KO and WT. (B–D) Thrombotic challenge in WT (n = 13) and iPLA$_2$γ-KO mice (n = 12). (B and C) Histological examination of lungs from (B) WT and from (C) iPLA$_2$γ-KO mice killed 2 min after injection of 0.25 mg/kg collagen and 20 mg/kg epinephrine mixure. Representative results of at least three experiments are shown. (D) Data represent percentage of deaths within 1 hr after injection of collagen and epinephrine mixure. P values were determined by Fisher's exact test: *P<0.05 between iPLA$_2$γ-KO (n = 12) and WT (n = 13). (E) Serum TXB$_2$ content after injection of collagen and epinephrine mixture. Data are mean±SEM. *P<0.05 between iPLA$_2$γ-KO (n = 3) and WT (n = 6).
doi:10.1371/journal.pone.0109409.g007

serum from iPLA$_2$γ-KO mice after injection were significantly lower than those from WT mice (Figure 7E). These results suggest that iPLA$_2$γ plays an important role in *in vivo* TXA$_2$ production accompanied by thrombus formation.

Discussion

PLA$_2$ plays a central role in platelet activation by hydrolysis of membrane phospholipids in response to a variety of stimuli. Previous studies have shown that, among several different PLA$_2$ enzymes, cPLA$_2$α is critical for platelet activation, even though other PLA$_2$(s) may also be involved [10]. The present study has revealed that iPLA$_2$γ, one of the Ca^{2+}-independent intracellular PLA$_2$ enzymes, represents the missing link; it is also responsible for stimulus-dependent AA release and functions as a key enzyme in platelet aggregation *in vitro* and thrombus formation *in vivo*. Only the metabolic roles of iPLA$_2$γ have thus far been highlighted *in vivo* [23,27,32]. This is the first demonstration that iPLA$_2$γ has a previously unrecognized homeostatic role in a particular lineage of hematopoietic cells, namely platelets.

When WT platelets were stimulated with ADP, breakdown of PE (plasmalogen-type) and PG-bearing AA at the *sn*-2 position was obvious (Figures 5). In sharp contrast, the amounts of these PE subclasses were unaffected by ADP stimulation in iPLA$_2$γ-deficient platelets. In addition to the release of AA, the production of TXA$_2$ was also reduced by iPLA$_2$γ deficiency (Figure 4). These results suggest that in mouse platelets, iPLA$_2$γ is activated in ADP-stimulated platelets and selectively hydrolyzes AA-containing plasmalogen-PE to release AA, leading to the production of TXA$_2$. The production of other AA metabolites, such as 12*(S)*-HETE, PGE$_2$ and PGD$_2$ also tended to be reduced in iPLA$_2$γ-KO mouse platelets. iPLA$_2$γ might be preferentially coupled with COX-1-TXA$_2$ synthase pathway but a portion of iPLA$_2$γ-liberated AA might be utilized by the other metabolic pathway. By comparison, in cPLA$_2$α-deficient platelets, ADP-induced TXA$_2$ generation remained entirely intact and collagen-induced TXA$_2$ generation was reduced by only half [10]. This implies that, at least under these particular stimuli, iPLA$_2$γ could account largely, if still not solely, for the TXA$_2$ pool produced independently of cPLA$_2$α. It should be noted that the levels of several PG subclasses tended to be lower in iPLA$_2$γ-deficient platelets than in WT platelets, even in the absence of stimuli (Figure 5A). The lower levels of these PG subclasses might lead to reduction in hydrolysis of PG in response to collagen, as well as to ADP. Cardiolipin and its precursor PG are mostly confined to mitochondrial membranes. Levels of both cardiolipin and PG were reduced in the heart, brain and skeletal muscle of the iPLA$_2$γ-deficient mice [23,29,32]. iPLA$_2$γ has been reported to be localized in the mitochondria, peroxisomes and ER of several cells [20,27]. In mouse platelets, iPLA$_2$γ may be involved in the maintenance of mitochondrial membranes through membrane remodeling, as well as stimulus-dependent hydrolysis of phospholipids. However, mitochondrial morphology and activity (as monitored by ATP synthesis) appeared to be intact in iPLA$_2$γ-deficient platelets, underscoring a difference from the profound effects of iPLA$_2$γ deficiency on mitochondrial homeostasis in brain, heart and skeletal muscle [22,29,32].

Selective hydrolysis of plasmalogen-type phospholipids in response to thrombin, collagen or U46619 has also been reported in human platelets [12]. Human platelets express both iPLA$_2$β and iPLA$_2$γ; in that they differ from mouse platelets, in which iPLA$_2$γ is dominant. Amounts of arachidonylated plasmenylcholine and plasmalogen species were significantly decreased by thrombin stimulation in human platelets. It was also shown that pretreatment with the iPLA$_2$γ-specific inhibitor *R*-BEL inhibited these thrombin-stimulated phospholipid hydrolyses more effectively than iPLA$_2$β inhibitor *S*-BEL [12]. Our previous experiments found that overexpression of iPLA$_2$γ caused reduction in AA-containing plasmalogen subclasses in HEK293 cells [20]. Thus, activated iPLA$_2$γ appears to selectively hydrolyze AA-containing plasmalogen-type phospholipids not only in mouse platelets but also in several tissues and cells including human platelets. In mouse platelets, ADP- or collagen-induced TXA$_2$ generation was reduced by iPLA$_2$γ deficiency, although its generation in response

to other stimuli such as thrombin was unaffected (Figure 4). There was no difference in hydrolysis of plasmalogen PE in response to collagen between WT and iPLA$_2\gamma$-deficient platelets (Figure 5B). Agonist-dependent activation mechanism of iPLA$_2\gamma$ might be different between human and mouse platelets.

Furthermore, in this study we found that among the agonists tested, only ADP-induced platelet aggregation was reduced by iPLA$_2\gamma$ deficiency (Figure 2). Although TXA_2 generation induced by ADP or collagen was reduced (Figure 4), aggregation in response to stimuli other than ADP, including collagen, was not affected. It has been reported that there are TXA_2-dependent and -independent pathways in platelet aggregation [33,34]. As iPLA$_2\gamma$-deficient platelets could fully aggregate in response to AA and U46619 (Figure 2), the TXA_2-dependent aggregation pathway was not affected by iPLA$_2\gamma$ deficiency. Our experiments using the $P2Y_1$ agonist and antagonist showed that iPLA$_2\gamma$ is involved in $P2Y_1$-mediated platelet aggregation (Figure 3D and E). Although $P2Y_1$ is coupled with G_q and its activation leads to Ca^{2+} mobilization [29], iPLA$_2\gamma$ deficiency did not affect ADP-induced increment in intracellular Ca^{2+} levels through G_q-coupled $P2Y_1$ receptor (Figure 3G) Intraplatelet crosstalk between iPLA$_2\gamma$ activation and Ca^{2+} mobilization may regulate ADP-induced aggregation.

It is noteworthy that mice lacking iPLA$_2\gamma$ have prolonged bleeding times and are resistant to thromboembolism induced by injection of epinephrine and collagen, as is the case with cPLA$_2\alpha$-deficient mice [10]. These results indicate that iPLA$_2\gamma$ plays a critical role in platelet hemostasis and thrombus formation *in vivo*, although iPLA$_2\gamma$ deletion did not affect *in vitro* platelet aggregation in response to platelet activators other than ADP. As inappropriate thrombus formation could lead to acute coronary syndromes and progression of atherosclerotic disease, antithrombotic drugs are used for prevention and therapy for these diseases. Three classes of inhibitors of platelet aggregation have demonstrated substantial clinical benefits. Aspirin acts by irreversibly inhibiting COX-1, and therefore blocking the synthesis of TXA_2. The indirect-acting (ticlopidine, clopidogrel, prasugrel) and direct-acting (ticagrelor) antagonists of $P2Y_{12}$ block the thrombus-stabilizing activity of ADP. Parenteral GPIIb/IIIa inhibitors directly block platelet-platelet interactions. Despite well-established benefits, all of these antiplatelet agents have important limitations. iPLA$_2\gamma$ has proven to be a potential target for antithrombotic drug development.

Acknowledgments

We thank Prof. Koji Eto (Center for iPS Cell Research and Application, Kyoto University) for helpful discussions, and Ms. M. Kawai and Ms. A. Kudo for their technical assistance.

Author Contributions

Conceived and designed the experiments: EY HS MM SH. Performed the experiments: EY KR MO YT HS. Analyzed the data: EY HK HS YN MM SH. Contributed reagents/materials/analysis tools: HS HK MM. Contributed to the writing of the manuscript: EY MM SH.

References

1. Broos K, Feys HB, De Meyer SF, Vanhoorelbeke K, Deckmyn H (2011) Platelets at work in primary hemostasis. Blood Rev 25: 155–167.
2. Packham MA (1994) Role of platelets in thrombosis and hemostasis. Can J Physiol Pharmacol 72: 278–284.
3. Cimmino G, Golino P (2013) Platelet biology and receptor pathways. J Cardiovasc Transl Res 6: 299–309.
4. Nakahata N (2008) Thromboxane A_2: physiology/pathophysiology, cellular signal transduction and pharmacology. Pharmacol Ther 118: 18–35.
5. Shen RF, Tai HH (1998) Thromboxanes: synthase and receptors. J Biomed Sci 5: 153–172.
6. Yeung J, Holinstat M (2011) 12-lipoxygenase: a potential target for novel anti-platelet therapeutics. Cardiovasc Hematol Agents Med Chem 9: 154–164.
7. Johnson EN, Brass LF, Funk CD (1998) Increased platelet sensitivity to ADP in mice lacking platelet-type 12-lipoxygenase. Proc Natl Acad Sci U S A 95: 3100–3105.
8. Kudo I, Murakami M (2002) Phospholipase A_2 enzymes. Prostaglandins Other Lipid Mediat 68–69: 53–58.
9. Bartoli F, Lin HK, Ghomashchi F, Gelb MH, Jain MK, et al. (1994) Tight binding inhibitors of 85-kDa phospholipase A_2 but not 14-kDa phospholipase A_2 inhibit release of free arachidonate in thrombin-stimulated human platelets. J Biol Chem 269: 15625–15630.
10. Wong DA, Kita Y, Uozumi N, Shimizu T (2002) Discrete role for cytosolic phospholipase $A_2\alpha$ in platelets: studies using single and double mutant mice of cytosolic and group IIA secretory phospholipase A_2. J Exp Med 196: 349–357.
11. Lehr M, Griessbach K (2000) Involvement of different protein kinases and phospholipases A_2 in phorbol ester (TPA)-induced arachidonic acid liberation in bovine platelets. Mediators Inflamm 9: 31–34.
12. Beckett CS, Kell PJ, Creer MH, McHowat J (2007) Phospholipase A_2-catalyzed hydrolysis of plasmalogen phospholipids in thrombin-stimulated human platelets. Thromb Res 120: 259–268.
13. Baulande S, Langlois C (2010) Proteins sharing PNPLA domain, a new family of enzymes regulating lipid metabolism. Med Sci 26: 177–184.
14. Murakami M, Taketomi Y, Miki Y, Sato H, Hirabayashi T, et al. (2011) Recent progress in phospholipase A_2 research: from cells to animals to humans. Prog Lipid Res 50: 152–192.
15. Balsinde J, Dennis EA (1997) Function and inhibition of intracellular calcium-independent phospholipase A_2. J Biol Chem 272: 16069–16072.
16. Franchi L, Chen G, Marina-Garcia N, Abe A, Qu Y, et al. (2009) Calcium-independent phospholipase $A_2\beta$ is dispensable in inflammasome activation and its inhibition by bromoenol lactone. J Innate Immun 1: 607–617.
17. Ackermann EJ, Conde-Frieboes K, Dennis EA (1995) Inhibition of macrophage Ca^{2+}-independent phospholipase A_2 by bromoenol lactone and trifluoromethyl ketones. J Biol Chem 270: 445–450.
18. Akiba S, Sato T (2004) Cellular function of calcium-independent phospholipase A_2. Biol Pharm Bull 27: 1174–1178.
19. Balsinde J, Balboa MA, Dennis EA (1997) Antisense inhibition of group VI Ca^{2+}-independent phospholipase A_2 blocks phospholipid fatty acid remodeling in murine $P388D_1$ macrophages. J Biol Chem 272: 29317–29321.
20. Murakami M, Masuda S, Ueda-Semmyo K, Yoda E, Kuwata H, et al. (2005) Group VIB Ca^{2+}-independent phospholipase $A_2\gamma$ promotes cellular membrane hydrolysis and prostaglandin production in a manner distinct from other intracellular phospholipases A_2. J Biol Chem 280: 14028–14041.
21. Kuwata H, Fujimoto C, Yoda E, Shimbara S, Nakatani Y, et al. (2007) A novel role of group VIB calcium-independent phospholipase A_2 (iPLA$_2\gamma$) in the inducible expression of group IIA secretory PLA_2 in rat fibroblastic cells. J Biol Chem 282: 20124–20132.
22. Yan W, Jenkins CM, Han X, Mancuso DJ, Sims HF, et al. (2005) The highly selective production of 2-arachidonoyl lysophosphatidylcholine catalyzed by purified calcium-independent phospholipase $A_2\gamma$: identification of a novel enzymatic mediator for the generation of a key branch point intermediate in eicosanoid signaling. J Biol Chem 280: 26669–26679.
23. Yoda E, Hachisu K, Taketomi Y, Yoshida K, Nakamura M, et al. (2010) Mitochondrial dysfunction and reduced prostaglandin synthesis in skeletal muscle of Group VIB Ca^{2+}-independent phospholipase $A_2\gamma$-deficient mice. J Lipid Res 51: 3003–3015.
24. Moon SH, Jenkins CM, Liu X, Guan S, Mancuso DJ, et al. (2012) Activation of mitochondrial calcium-independent phospholipase $A_2\gamma$ (iPLA$_2\gamma$) by divalent cations mediating arachidonate release and production of downstream eicosanoids. J Biol Chem 287: 14880–14895.
25. Bligh EG, Dyer WJ (1959) A rapid method of total lipid extraction and purification. Can J Biochem Physiol 37: 911–917.
26. Kuwata H, Yoshimura M, Sasaki Y, Yoda E, Nakatani Y, et al. (2013) Role of long-chain acyl-coenzyme A synthetases in the regulation of arachidonic acid metabolism in interleukin 1β-stimulated rat fibroblasts. Biochim Biophys Acta 1841: 44–53.
27. Mancuso DJ, Kotzbauer P, Wozniak DF, Sims HF, Jenkins CM, et al. (2009) Genetic ablation of calcium-independent phospholipase $A_2\gamma$ leads to alterations in hippocampal cardiolipin content and molecular species distribution, mitochondrial degeneration, autophagy, and cognitive dysfunction. J Biol Chem 284: 35632–35644.
28. Gachet C (2008) P2 receptors, platelet function and pharmacological implications. Thromb Haemost 99: 466–472.
29. Kahner BN, Shankar H, Murugappan S, Prasad GL, Kunapuli SP (2006) Nucleotide receptor signaling in platelets. J Thromb Haemost 11: 2317–2326.
30. Lenain N, Freund M, Léon C, Cazenave JP, Gachet C (2003) Inhibition of localized thrombosis in $P2Y_1$-deficient mice and rodents treated with MRS2179, a $P2Y_1$ receptor antagonist. J Thromb Haemost 1: 1144–1149.

31. Léon C, Hechler B, Freund M, Eckly A, Vial C, et al. (1999) Defective platelet aggregation and increased resistance to thrombosis in purinergic $P2Y_1$ receptor-null mice. J Clin Invest 104: 1731–1737.
32. Mancuso DJ, Sims HF, Han X, Jenkins CM, Guan SP, et al. (2007) Genetic ablation of calcium-independent phospholipase $A_2\gamma$ leads to alterations in mitochondrial lipid metabolism and function resulting in a deficient mitochondrial bioenergetic phenotype. J Biol Chem 282: 34611–34622.
33. Stalker TJ, Newman DK, Ma P, Wannemacher KM, Brass LF (2012) Platelet signaling. Handb Exp Pharmacol 210: 59–85.
34. Thomas DW, Mannon RB, Mannon PJ, Latour A, Oliver JA, et al. (1998) Coagulation defects and altered hemodynamic responses in mice lacking receptors for thromboxane A_2. J Clin Invest 102: 1994–2001.